The Journal of Experimental Medicine

Functional Heterogeneity of Marginal Zone B Cells Revealed by Their Ability to Generate Both Early Antibody-forming Cells and Germinal Centers with Hypermutation and Memory in Response to a T-dependent Antigen

Haifeng Song and Jan Cerny

Department of Microbiology and Immunology, University of Maryland, School of Medicine, Baltimore, MD 21201

Abstract

Marginal zone (MZ) B cells play a major role in the first-line responses against blood-born T-independent bacterial antigens (TI), but the full scope of their immune functions is not known. Here we compare the responses of MZ and follicular (FO) B cells to a T-dependent antigen (TD), hapten–(4-hydroxy-3-nitrophenyl)acetyl (NP) coupled to chicken γ-globulin, in a cell transfer system. Consistent with the conventional paradigm, MZ B cells but not FO B cells rapidly generated the early burst of NP-specific antibody-forming cells (AFC), high levels of IgM Ab, and early IgG with relatively high affinity to NP. However, MZ B cells were also capable of forming germinal centers (GCs) albeit with a delay, compared with FO B cells. The early AFCs and the GCs originated from different MZ precursors, but the MZ- and FO-derived GCs were similar in V_H gene repertoire, somatic mutation, and production of late AFC and IgG Ab. Surprisingly, the MZ but not the FO memory response included IgM Ab. We conclude that MZ B cells are heterogeneous, comprising cells for both early AFC response and GC/memory pathway against TD antigens.

Key words: B cells • marginal zone • T-dependent Ag • antibody-forming cells • germinal center

Introduction

Newly formed B cells in adults migrate from BM to peripheral lymphoid tissues where they continue to differentiate into functionally and anatomically distinct subsets (1). Mature peripheral B cells include B1 cells, which reside mainly in peritoneal and pleural cavities (2), and the conventional B2 B cells. The mature B2 cell population is heterogeneous, consisting of the major follicular B cells (FO), in LN and splenic lymphoid follicles, and a subset residing in the marginal zone (MZ) of the spleen (3). MZ and FO B cells are distinguished by differential expression of several cell surface markers: MZ B cells are $IgD^{low}CD21^{high}CD23^{low/-}$, whereas FO B cells are $IgD^{high}CD21^{inter}CD23^{high}$ (4, 5). In addition, MZ B cells express various activation markers, such as high basal levels of CD80, CD86, CD40, and CD44, and low level of CD62L (5, 6). As a functional corollary, MZ B cells exhibit rapid and robust proliferation and Ig secretory responses to stimulation with LPS, anti-IgM, and CD40 ligands (5–7). The apparent hyperreactivity of MZ B cells and their unique anatomic localization at the red pulp junction strongly suggest that these B cells mediate rapid Ab responses to blood-born antigens (8).

There is increasing evidence for selection of B cells into the MZ or follicular pool through B cell receptor (BCR)–mediated signals (9, 10). Studies on transgenic mice demonstrated that B cells expressing BCR with specificity for different Ags had accumulated either in the follicles or in the MZ (11). In particular, B cells specific for the bacterial epitope, phosphorylcholine, homed to MZ and responded to the TI form of the Ag (3, 11). The ligands that control cellular selection and homing are not known (3). Interestingly, in humans (12, 13), and to a lesser extent in rats (14), some MZ B cells express somatically mutated IgV genes, suggesting

Address correspondence to Jan Cerny, Dept. of Microbiology and Immunology, University of Maryland, School of Medicine, 655 West Baltimore St., Rm. 13-015 BRB, Baltimore, MD 21201-1559. Phone: (410) 706-7114; Fax: (410) 706-2129; email: ojone002@umaryland.edu

Abbreviations used in this paper: AFC, antibody-forming cell; BCR, B cell receptor; CGG, chicken gammaglobulin; CSR, class-switch recombination; DN, double negative; FO, follicular; GC, germinal center; HRP, horseradish peroxidase; MZ, marginal zone; NIP, 4-hydroxy-5-iodo-3-nitrophenyl acetyl; NP, (4-hydroxy-3-nitrophenyl)acetyl; PALS, periarteriolar lymphoid sheath; PNA, peanut agglutinin; R/S, replacement to silent; SA-ALPH, Streptavidin conjugated to alkaline phosphatase; SHM, somatic hypermutation; TD, T-dependent Ag; TI, T-independent Ag; TI-I, TI type I Ag; TI-II, TI type II Ag.

 J. Exp. Med. © The Rockefeller University Press • 0022-1007/2003/12/1923/13 $8.00
Volume 198, Number 12, December 15, 2003 1923–1935
http://www.jem.org/cgi/doi/10.1084/jem.20031498

that they already encountered Ags and became memory cells. Collectively, these findings suggest that the repertoire of MZ B cells is skewed by stimulation with environmental Ags.

Fagarasan and Honjo (15) proposed that MZ B cells respond to T-independent Ags (TI) and may not be regulated by T cells. This notion was based primarily on the phenotype of Pyk-2–deficient mice (16) that had a severely reduced MZ B cell population and diminished Ab response to TI type I Ag (TI-I) and TI type II Ag (TI-II). However, this defect was restricted only to the IgG2a and IgG3 isotypes, whereas IgG1 and IgG2b Ab responses to TI-I and TI-II Ags were unaffected. Moreover, the disruption of Pyk-2 also inhibited the IgM response to T-dependent Ags (TD). These conflicting observations suggest that the function of MZ B cells and their relationship with T cells are complex. Indeed, Tanigaki et al. (17) failed to find a relationship between MZ B cells and TI Ab responses. They generated mice lacking expression of RBP-J, a mediator of Notch signaling, in B cells using conditional mutagenesis. Such mice had no MZ B cells, but Ab responses to TI-I, TI-II, and TD Ag were unaffected.

The phenotypes of the Pyk-2 (16) and RBP-J (17) mutants have shown that MZ B cells are not dedicated only to TI Ab responses. MZ B cells present Ags and deliver costimulatory signals to T cells more efficiently than FO B cells in vitro (5), suggesting that MZ cells can mount rapid Ab responses requiring cognate T cell help (18). Indeed, using a hapten-carrier system, Liu et al. (19) demonstrated a rapid appearance of specific, hapten-binding MZ B cells in rats that had been primed previously to the carrier protein.

We hypothesized that the Ab response of MZ B cells to TD Ags is qualitatively different from that of FO B cells and that the two cell subsets differ in their potential to form antibody-forming cells (AFC), germinal centers (GCs), and memory cells. To test this prediction rigorously, we reconstituted *scid* mice with purified MZ and FO B cells from naive WT C57BL/6 donors, supplemented them with carrier-primed T cells, and then stimulated the chimeras with the hapten-(4-hydroxy-3-nitrophenyl)acetyl (NP) coupled to chicken gammaglobulin (CGG). The NP-specific Ab response of Igh^b mice has been well characterized at the cellular and molecular level: NP-binding V_H regions are encoded by the group of V186.2/V3 genes of the J558 family; the dominant clonotype expresses the V186.2 segment rearranged to DFL16.1/2 and J_H2 segments in combination with the λ L chain (20–23). This response to NP thus provides a precise tool for comparing potential differences between MZ and FO B cells in repertoire and function. Our results show an unexpected functional heterogeneity of MZ B cells. Upon stimulation with TD Ag, MZ cells rapidly produce large numbers of AFC that have distinct clonotypic repertoire; however, these cells also give rise to GCs with characteristic somatic hypermutation and generate immunological memory.

Materials and Methods

Animals. Normal C57BL/6, B6.SJL-Ly5.1 (CD45.1) (both 8–12 wk), and C57BL/6 *scid* mice (8–10 wk) were purchased from The Jackson Laboratories and maintained in microisolator cages in the animal facility of the University of Maryland, Baltimore.

Antigens. NP and its analogue (4-hydroxy-5-iodo-3-nitrophenyl)acetyl (NIP) (Cambridge Research Biochemical) were conjugated at various substitution ratios to CGG (Sigma-Aldrich) or BSA (Amersham Biosciences) as described (24).

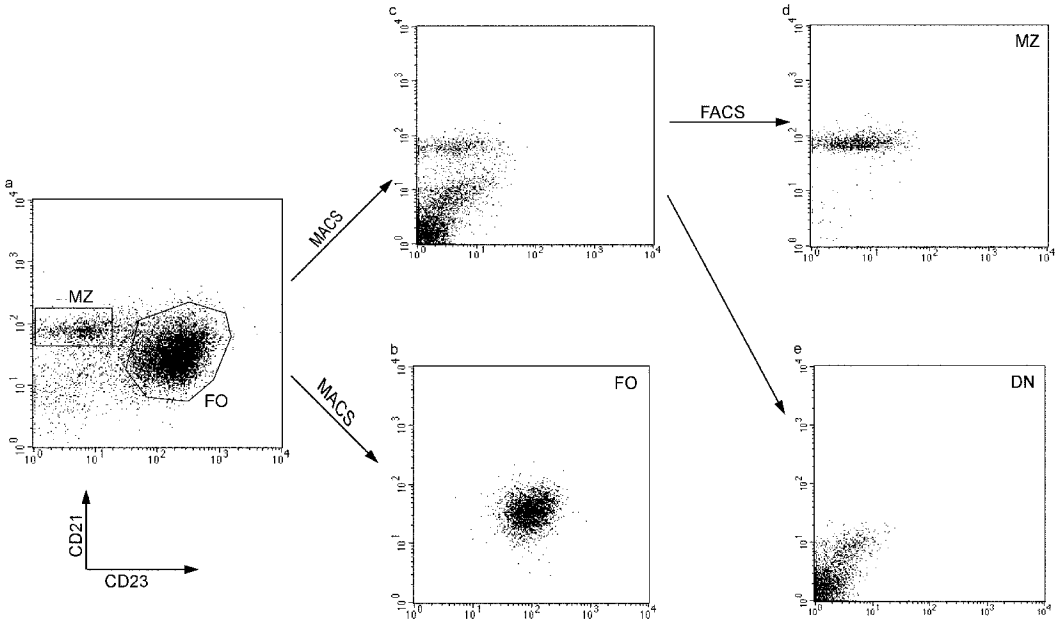

Figure 1. Purification of splenic MZ and FO B cells. (a) T cell–depleted splenocytes were stained for CD21-FITC and CD23-PE, and the $CD23^{hi}$ FO cells were separated by autoMACS with anti-PE beads (b). The $CD23^-$ fraction (c) was stained with B220-APC, and the $B220^+CD21^{hi}$ MZ cells (d) were separated by FACS® from the $CD21^-$ $CD23^-$ DN fraction (e). The FO and MZ B cell fractions were reanalyzed before the cell transfer (b and d).

Antibodies. Anti-Thy1.2 (HO13–4), anti-CD4 (GK1.5), and anti-CD8 (3.155) hybridomas (American Type Culture Collection), and anti-CD3 hybridoma (145–2C11, provided by Dr. Jeffrey A. Bluestone, University of California, San Francisco, CA) were grown in our laboratory, and the Abs were isolated from culture supernatants by salt precipitation. Anti–B220-APC (RA-6B2), anti–CD23-PE (B3B4), anti–CD21-FITC (7G6), anti–CD19-PE (1D3), anti–CD11b-biotin (M1/70), anti–CD11c-biotin (HL3), anti–CD45.2-biotin (104), anti–CD45.1-biotin (A20), and GL-7-FITC were purchased from BD Biosciences. Horseradish peroxidase (HRP)-conjugated goat anti–mouse IgM, IgG, IgG1, IgG2a, IgG2b, IgG3, λ, and κ were obtained from Southern Biotechnology Associates, Inc.

Purification of MZ, FO B Cells. Single spleen cell suspensions were prepared by grinding spleens between two frosted glass slides in medium consisting of RPMI 1640 with 25 mM Hepes (Life Technologies) and 0.5% BSA (Sigma-Aldrich). B cell–enriched populations were prepared by depleting T cells using two treatments with an antibody cocktail consisting of anti-CD4 (GK1.5), anti-CD8 (3.155), anti-Thy1.2 (HO-13–4), and normal rabbit serum, at 37°C for 40 min. The enriched B cells were stained with anti–CD23-PE on ice for 15 min followed by incubating with anti-PE microbeads (Miltenyi Biotec), and the $CD23^+$ B cells (FO B cells) were separated from the $CD23^-$ B cells by autoMACS (Miltenyi Biotec). The $CD23^-$ B cells were further stained with anti–CD21-FITC and B220-APC, and the CD21-high, B220-positive MZ B cells were purified by FACS® sorting (Moflo, DakoCytomation). The purity of FO B cells and MZ B cells was >97 and 95%, respectively (Fig. 1).

CD4 T Cell Preparation. T cells were enriched by passing splenocytes from CGG-primed C57BL/6 mice through nylon wool (Wako BioProducts) columns according to the protocol recommended by the manufacturer. The enriched T cells were incubated with anti–B220-PE, anti–CD8-PE, anti–CD19-PE, anti–$I\text{-}A^b$-biotin, anti–CD11b-biotin on ice for 15 min followed by incubating with Streptavidin microbeads and anti–PE microbeads at 4°C for 15 min. The CD4 T cells were purified by passing the above-stained cell suspension through a MACS LS column (Miltenyi Biotec). The resulting CD4 T cells contained <1% of CD8 T cells and B220-positive B cells.

Adoptive Transfer and Immunization. ~2–2.5 × 10^6 of purified MZ or FO B cells, together with 4 × 10^6 CGG-primed CD4 T cells were injected i.v. into C57BL/6 *scid* mice, and the recipients were immunized i.p. with 40 μg of NP-CGG in alum. Blood and/or spleen samples were collected for analysis of the primary response at days 4, 8, 14, 36, 60, and 85. To measure memory responses, splenocytes from the recipient mice were collected at day 85 after primary immunization, and 5 × 10^6 cells were transferred into *scid* mice. The mice were challenged with 10 μg of soluble NP-CGG i.p., and memory responses were examined at days 6 and 9 after the boost. The *scid* recipients that were not challenged, and the recipients of naive splenocytes that received the boost dose of soluble Ag served as controls.

In experiments with mixed B cells subsets, MZ cells were prepared from C57BL/6 mice expressing the Ly5.2 allele of the common leukocyte antigen CD45, whereas the FO cells and the $CD21^{lo}CD23^-$ (labeled as "double negative") B cells were from BL6. SJL-Ly5.1 (CD45.1) donors.

Antibody Measurement. Serum NP-specific Abs were measured by standard ELISA using 96-well plates coated with 100 μg/ml of NIP_{18}-BSA. The relative affinity of serum Ab was determined by titration on ELISA plates coated with BSA coupled to NIP at different ratios, respectively, NIP_4-BSA and NIP_{18}-BSA. The plates were developed with HRP-conjugated goat Ab specific for mouse IgG_1 that is the major isotype of anti-NP Ab (>80% of IgG) in this system. Binding (OD450) to each plate at the linear portion of the titration curve was determined, and the relative affinity of Ab was expressed by binding to NIP_4-BSA as a percentage of binding to NIP_{18}-BSA (Eq. 1):

$$\text{affinity} = \frac{OD450w.NIP_4BSA \times 100}{OD450w.NIP_{18}BSA}. \quad (1)$$

Phenotypic Analysis of GC B Cells by FACS®. Mice were killed at 14 d after the cell transfer and immunization, and the splenocyte suspension was stained with anti–CD19-PE, GL-7–FITC, and biotinylated anti-CD45.2 (Ly5.2) or anti-CD45.1 (Ly5.1) followed by SA-APC. GC B cells were enumerated as $GL\text{-}7^+/Ly5.1^+$ or $GL\text{-}7^+/Ly5.2^+$ cells within the CD19 gate.

Immunohistochemical Staining of GC and AFC and Microdissection of Target Cells. Frozen splenic sections were prepared and stained as described previously (25). The specific, NP-reactive GCs were identified by dual staining with peanut agglutinin (PNA) coupled to horseradish peroxidase (PNA-HRP) (EY Laboratories, Inc.) in combination with a biotinylated NIP-BSA followed by Streptavidin conjugated to alkaline phosphatase (SA-ALPH) (ImmunoPure). NP-specific AFCs were visualized as plasmacytes stained with biotinylated NIP-BSA. These cells formed typical foci close to the borders of B cell follicles. PNA^+NIP^+ GC cells and NIP-positive AFC foci were recovered using a sharpened micropipette controlled by micromanipulator (model MM188; Nikon). The recovered cells were lysed with PCR-lysing buffer (1× PCR buffer containing 100 μg/ml proteinase K, 0.05% Tween 20) at 56°C for 1 h followed by inactivation of proteinase at 95°C for 10 min. Resulting samples were used for PCR amplification.

In mice reconstituted with cells expressing different CD45 alleles, the GCs in splenic sections were visualized by dual staining with PNA-HRP and anti–Ly5.1-biotin plus SA-ALPH. The dual-stained PNA^+ $Ly5.1^+$ GCs were readily distinguishable from single-stained $PNA^+Ly5.1^-$ GCs in the same section (see Fig. 4 in Results), and the latter were then scored as $Ly5.2^+$. The anti-Ly5.2 conjugate could not be used for identification of GCs in sections because of the high background staining.

PCR Amplification, V_H Gene Repertoire Screening, and Mutation Analysis. Amplification of VDJ rearrangements using two pairs of primers for nested PCR was performed as described previously (25, 26). PCR products were cloned using pBluescriptSKII plasmid (Stratagene) and DH5α *Escherichia coli* and screened by hybridization with V_H gene–specific, ^{32}P-labeled oligonucleotides (26). All transformed colonies hybridized with the probe (5′-GTAGCCAGAAGCCTTGCAGGA-3′) corresponding to the region of genomic DNA (aa position 21–27) that is shared by the V186.2/V3 group of 22 genes of the J558 family. A proportion of these colonies also hybridized with the probe (5′-TACCACCACTATTAGGATCAATCCT-3′), which identifies a DNA region (aa position 50–57) specific for the V186.2 gene sequence. The number of $21\text{–}27^+/50\text{–}57^-$ colonies has been shown to correlate with the number of B cells expressing one of the analogue (non-V186.2) genes of the V186.2/V3 group (26). Plasmid DNA from the double-positive ($21\text{–}27^+/50\text{–}57^+$) colonies was extracted and sequenced by the Biopolymer Laboratory of the University of Maryland, School of Medicine using an automatic DNA sequencing system (Applied Biosynthesis). All double-positive colonies invariably yielded the rearranged V186.2 sequence. Mutations were scored based on nucleotide substitutions in the V_H gene only.

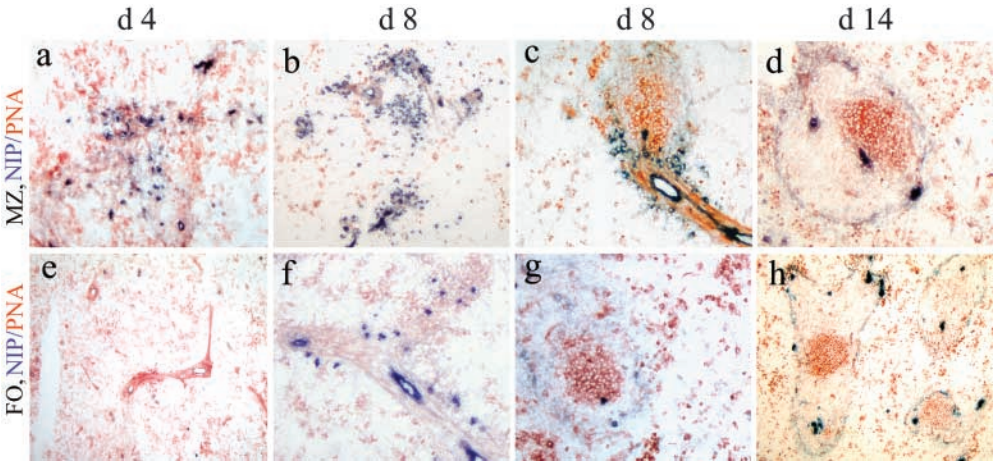

Figure 2. Visualization of NP-binding AFC (blue) and PNA$^+$ GC (red) in splenic sections from *scid* mice reconstituted with either MZ cells (a–d) or FO cells (e–h) plus carrier-primed T_H cells and immunized with NP-CGG/alum. Large foci of AFCs are seen in MZ cell recipients on day 4 (a) and 8 (b), whereas the FO cell recipients show a few scattered AFC on day 8 after the immunization (f). GC was rare in MZ mice on day 8 (c; GC, surrounded by AFC in dark blue) but became frequent and large on day 14 (d). Typical GCs were present in FO mice on day 8 (g) and 14 (h).

Shared mutations within a set of clonally related sequences (according to the CDR3) were counted as one mutational event.

Results

Distinct Cellular Responses of B Cell Subsets. *Scid* mice were reconstituted with either highly purified MZ cells ("MZ mice") or FO cells ("FO mice") plus carrier-primed T_H cells as described in Materials and Methods and Fig. 1. These recipients demonstrated marked differences in their responses to immunization with NP-CGG (Fig. 2). MZ mice exhibited an early extrafollicular AFC response with the appearance of NP-binding plasma cells on day 4 and large AFC foci formation by day 8 (Fig. 2, a and b), whereas the formation of the GC was relatively slower. Only few follicles stained faintly with PNA on day 8 (Fig. 2 c); PNA$^+$ GCs were seen in less than half of splenic sections, numbering less than three GCs/section (Table I). However, by day 14 the GCs in MZ mice reached typical size (Fig. 2 d) and numbered up to six per section (Table I). In contrast, FO mice had no AFC on day 4 (Fig. 2 e) and only few, scattered NP-binding plasmacytes were found on day 8 (Fig. 2 f); AFC foci were not seen until day 14 (not depicted). However, FO mice developed large PNA$^+$ GCs from day 8 (Fig. 2 g) that were apparent in every splenic section (Table I) and that continued on day 14 (Fig. 2 h).

Although the purity of MZ cells was >95% (Fig. 1 d), we considered the possibility that the GCs in MZ mice resulted from a small (~5–10%) cell contamination. Since the CD23$^+$ FO cells were removed by autoMACS before FACS® sorting for MZ cells, we considered that the most likely contamination was from the CD21^{lo}/CD23$^-$ double negative (DN) immature B cells (9) that might have completed their maturation to FO cells and form GCs after the adoptive transfer. We addressed this concern by reconstituting *scid* mice with purified Ly5.2$^+$ MZ cells (2.7×10^6) that were mixed with 3×10^5 cells from the CD21^{lo}/CD23$^-$ B cells (Fig. 1 e) that were isolated from Ly5.1$^+$

Table I. *Germinal Centers in the Spleen of Mice with MZ and FO B Cells*

Days postimmunization	B cells transferred	Spleen sections[a]	
		GC/section (range)	Positive/total[b]
8	MZ	0–3	10/21
		0–1	1/4
	FO	0–8	10/11
		1–4	14/14
14	MZ	0–6	5/10
		0–2	5/10
		0–1	3/9
		0–5	6/10
		0–3	9/14

[a]Serial longitudinal sections were prepared from two to three spleens/group (20–50 sections through ~50–60% of the splenic thickness). PNA$^+$ germinal centers were scored on several sections separated by ~20–30 μm.
[b]Positive sections contained at least one GC.

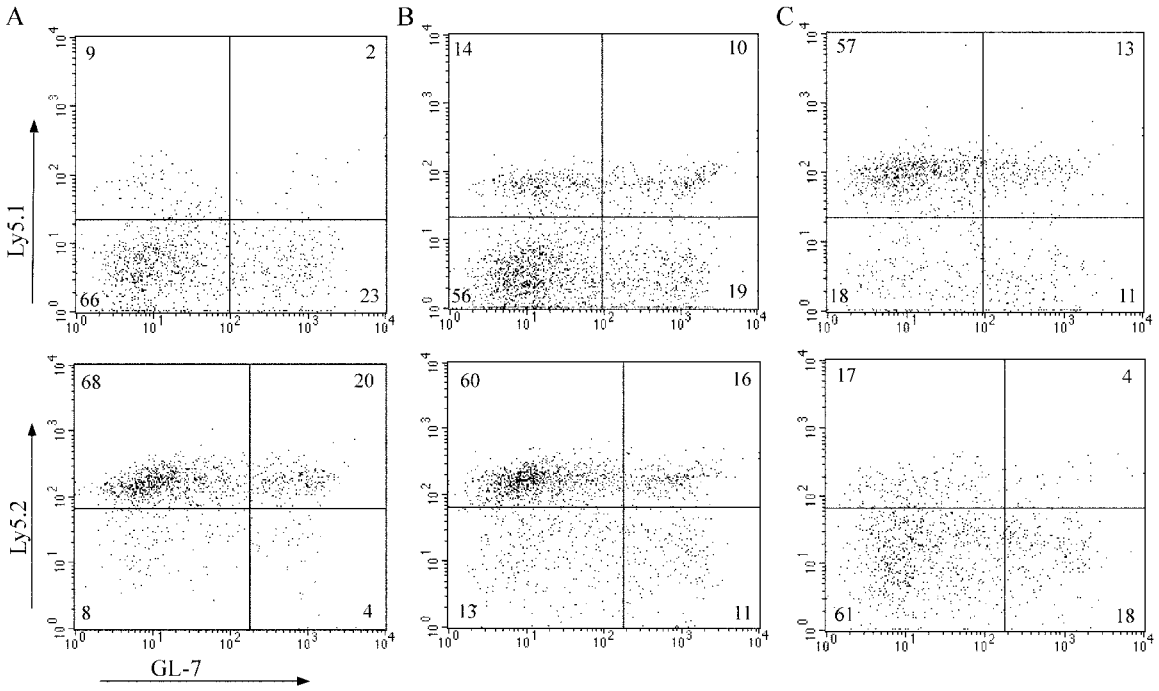

Figure 3. Enumeration of GL-7$^+$ GC B cells in day 14 spleen by costaining for Ly5.1 (top) or Ly5.2 (bottom) within CD19 gate. The numbers in top right corners show the percentage of CD19$^+$ Ly5.1$^+$ (or Ly5.2$^+$) cells that were GL-7 positive; the numbers in bottom right corners show the percentage of GL-7$^+$ B cells that did not express the allele. Groups of mice were reconstituted with B cell subsets of various ratios (numbers of cells are shown in Table II): (A) Ly5.2$^+$ MZ + Ly5.1$^+$ DN cells, 9:1; (B) Ly5.2$^+$ MZ + Ly5.1$^+$ FO, 9:1, and (C) Ly5.2$^+$ MZ + Ly5.1$^+$ FO, 1:9.

donors (see Materials and Methods). It should be emphasized that CD21 expression in the DN fraction is variable, with a few cells staining nearly as bright as the MZ cells (Fig. 1 c). Therefore, substantial numbers of GC B cells in these chimeras should be Ly5.1$^+$ if the GCs originated from the immature cells rather than MZ cells. However, at 14 d after the transfer and immunization, the numbers of GC B cells were nearly proportional to the input: 90% of GL-7$^+$ GC B cells were Ly5.2$^+$ by FACS® (Fig. 3 A, Table II, Group A), and all but one GC in splenic section were PNA$^+$/Ly5.1$^-$ (Table II, Group A). Thus, GCs in the MZ mice do not arise from immature B cells.

MZ Cells Form GCs in Competition with FO Cells. It could be argued that in normal spleen the potential of MZ

Table II. *Phenotypes of GC in Mice Reconstituted with MZ Plus FO and/or DN B Cells at Various Ratios*

				GC B cells in the recipient spleens[a]					
	Number of injected B cells			FACS® analysis (%)[b]			GC enumeration[c]		
Group	Ly5.2$^+$	Ly5.1+	Ratio (Ly5.2$^+$/Ly5.1$^+$)	Ly5.2$^+$GL-7$^+$	Ly5.1$^+$GL-7$^+$	Ratio (Ly5.2/Ly5.1)	Ly5.1$^-$PNA$^+$	Ly5.1$^+$PNA$^+$	Ratio (Ly5.1$^-$/Ly5.1$^+$)
	MZ	DN							
A	2.7×10^6	3×10^5	9:1	20	2	10	14.6 ± 5	1[d]	14
	MZ	FO							
B	2.7×10^6	3×10^5	9:1	16	10	1.6	17.4 ± 4.7	7.4 ± 3	2.4
	MZ	FO							
C	3×10^5	2.7×10^6	1:9	4	13	0.3	2.6 ± 1	12.6 ± 2.7	0.2

[a]Day 14 after adoptive transfer and immunization; three recipients/group.
[b]Pieces (~20%) of the spleens were pooled, stained, and gated on CD19 bright cells.
[c]Number of PNA$^+$ centers in 10 spleen sections; mean from three mice ± SD. See Materials and Methods and Fig. 4 for details on visualization of Ly5.1$^+$ and Ly5.1-GC.
[d]One PNA$^+$ center was found in one out of three mice.

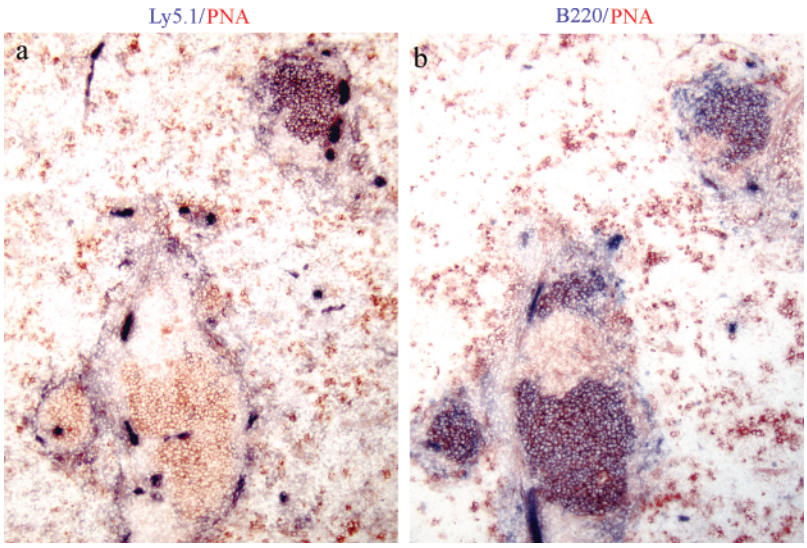

Figure 4. Phenotypes of day 14 germinal centers in splenic sections in mice reconstituted with Ly5.2$^+$ MZ cells (2.7×10^6) and Ly5.1$^+$ FO cells (3×10^5) plus T_H cells and immunized on the day of transfer. (a) Staining with PNA-HRP (red) and anti–Ly5.1-biotin plus SA-ALPH (blue) reveals one PNA$^+$Ly5.1$^+$ GC (purple) in the top right corner and two PNA$^+$Ly5.1$^-$ GC (red) in bottom section. (b) Adjacent section stained for PNA (red) and B220 (blue) demonstrates that the PNA$^+$ clusters are B cells.

cells to form GCs is eclipsed by a much larger population of FO cells. We examined this point by cotransferring the purified Ly5.2$^+$ MZ cells and Ly5.1$^+$ FO cells at ratios of 9:1 (group B) and 1:9 (group C) together with T_H cells. The numbers and the Ly5 phenotype of splenic GL-7$^+$ GC B cells at 14 d postimmunization were determined by FACS®, and the phenotypes of PNA$^+$ GCs in splenic sections were shown by costaining with anti-Ly5.1 as described in Materials and Methods. An example of the dual staining is shown in a splenic section from group B that contains three PNA$^+$ centers (Fig. 4 a): one dark purple GC in the top right corner is clearly Ly5.1$^+$/PNA$^+$, and two bright red GCs in the bottom left corner are PNA$^+$/Ly5.1$^-$ that were scored as Ly5.2$^+$. The scoring of GCs by this method was in general agreement with the FACS® analysis (Table II). GC B cells in the mixed chimeras were formed by either the Ly5.2$^+$ MZ cells or Ly5.1$^+$ FO cells, and their respective numbers vary according to the cellular input. Group B received nine times more Ly5.2$^+$ MZ cells than Ly5.1$^+$ FO cells (ratio 9:1), but the numbers of Ly5.2$^+$ GC B cells were only about twofold higher than Ly5.1$^+$ GC B cells as determined by either FACS® (Fig. 3 B) or by section staining (Table II). This is consistent with the notion that GC precursors in the FO cell subset are more frequent and/or robust compared with MZ B cells. However, this trend was not apparent when the MZ:FO input ratio was reversed to 1:9 in group C (Table II). The numbers of Ly5.2$^+$ GC B cells (Fig. 3 C) were nearly proportional to the input of Ly5.2$^+$ MZ cells. It is conceivable that these results were influenced by the mechanisms of homeostasis and cell expansion that may be different for MZ and FO subsets. Nevertheless, the results argue strongly that the GCs detected in MZ mice are not derived from contaminating FO cells.

Serum Antibody Responses. Consistent with the pattern of cellular responses in single-reconstituted animals, the MZ mice mounted a robust NP-specific IgM serum Ab response during the first week after the immunization (Fig. 5 a) and switched to IgG Ab on day 8 (Fig. 5 b). FO mice did not produce any detectable serum Ab until day 8; the level of IgM was 10-fold lower than in the MZ mice, whereas the IgG titers had a similar range among individual mice in both groups. Thus, the massive, early AFC formation in the MZ mice correlates well with the anti-NP IgM response. The origin of serum Ab in FO mice can be either from the dispersed plasmacytes (Fig. 2 f) or perhaps from B cells in the follicles, which might have secreted Ig without differentiation into typical plasmacytes. Interestingly, the MZ mice maintained 10-fold higher IgM Ab titers throughout the entire 2-mo period of observation, and as described below, they also displayed a brisk, recall IgM Ab response to the Ag boost. Each of the two independent experiments shown in Fig. 5 included groups of control mice reconstituted either with whole unseparated splenic B cell population together with purified T_H, or with T_H alone, and immunized with NP-CGG. Notably, mice with unseparated B cells maintained intermediate levels of IgM Ab relative to the MZ and FO mice, confirming that MZ B cells, which represent 5–10% of spleen B cells, make the major contribution to IgM responses. None of the mice from the control group reconstituted with only T cells produced detectable anti-NP serum Ab, demonstrating that neither a contaminating donor B cell population nor "leaky" host B cells contributed to the anti-NP responses (not depicted).

VD Gene Repertoire of Anti-NP Responses. The rearranged V_H genes in the NP-responding B cells in FO and MZ mice were examined by screening bacterial transformants with probes that discriminate between the V186.2 segment and the remaining "analogue genes" of the V186.2/V3 family. The V_H gene repertoire was expressed as the ratio between V186.2 and non-V186.2 (analogue) genes, and the rearranged V186.2/D/J segments were sequenced.

The most prominent finding in the MZ mice was the difference in the repertoire between the early AFC and the GC. Most AFCs (>70%) at day 8 used the V186.2 segment, but surprisingly few, if any, of those V_H genes were

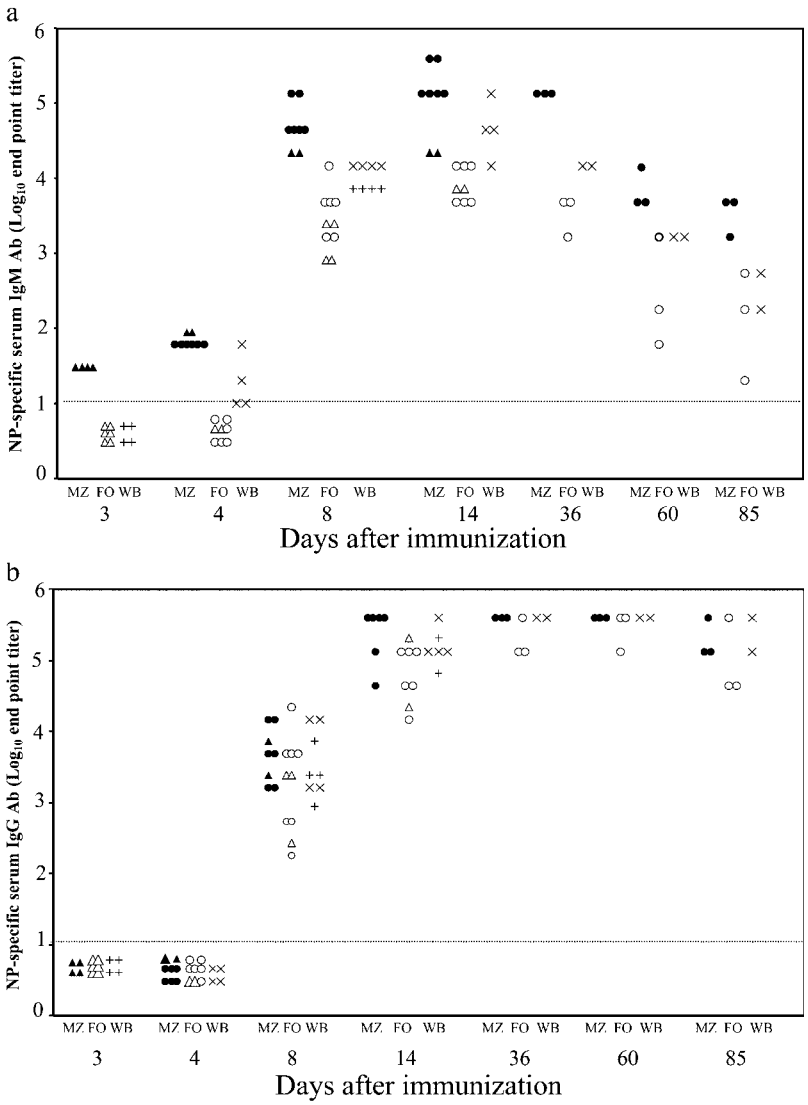

Figure 5. Kinetics of IgM (a) and IgG (b) serum Ab responses after single injection of 40 μg of NP-CGG/alum in mice reconstituted with purified MZ B cells (MZ, filled symbols), FO B cells (FO, open symbols), and whole splenic B cells (+ and ×) plus T_H cells. Each symbol represents one animal. Two independent experiments are shown using circles (● and ○), triangles (▲ and Δ) and different crosses (+ and ×). The points below the horizontal line represent negative sera (titer <1:10).

rearranged to the DFL16.1/2 segment (Fig. 6 a). Instead, the CDR3 was encoded by DSP 2–5, and other unidentified D genes and their length varied from 7 to 11 aa (Fig. 6 c). In contrast, the incipient GCs in MZ mice on day 8 were dominated by the non-V186.2 analogue genes; only 20% of GC B cells used the V186.2 segments, half of which were rearranged to DFL16.1/2 genes (Fig. 6 a). Unlike the early AFC repertoire, AFC recovered from MZ mice on day 14 expressed the canonical V186.2/DFL16.1/2 rearrangements (Fig. 6 a) with uniform CDR3 length (11–12 aa) (not depicted). Moreover, the repertoire of these late AFC was similar to that of the GC, and clones with identical CDR3 were found in both cell populations.

As expected, most of the V186.2 sequences recovered from early AFC foci in MZ mice were unmutated (27); only one focus contained somatically mutated AFC with an average of 1.2 mutations/V_H (Table III). It is unlikely that the mutated AFC originated from the rare, nascent GCs in MZ mice because the focus was microdissected from a splenic region devoid of PNA^+ follicles, and the VD gene repertoire of early AFC in these mice was very different from GC/late AFC repertoire. Thus, consistent with previous studies (21), the presence of mutations in early MZ AFCs suggests that some MZ B cells are immunologically experienced.

In FO mice, microdissection of the rare, early AFC for repertoire analysis was not technically feasible as they were not organized in foci (Fig. 2 f). However, ~50% of GC B cells on day 8 used the V186.2 segment, and this proportion increased further on day 14, which is typical of the repertoire of NP-reactive GCs in intact BL/6 mice (20). Approximately half of the V186.2 segments in FO GCs were rearranged to DFL16.1/2 (Fig. 6 b). Day 14 AFCs in these mice expressed a similar repertoire as the GC B cells and often shared CDR3 of uniform length (11–12 aa).

Somatic Hypermutation in GC and Late AFC. Studies have shown that immunocompromised mice (28, 30) or mice immunized with the bacterial epitope phosphorylcholine (28, 29) may develop GCs that appear to be morphologically normal but are deficient in somatic mutation

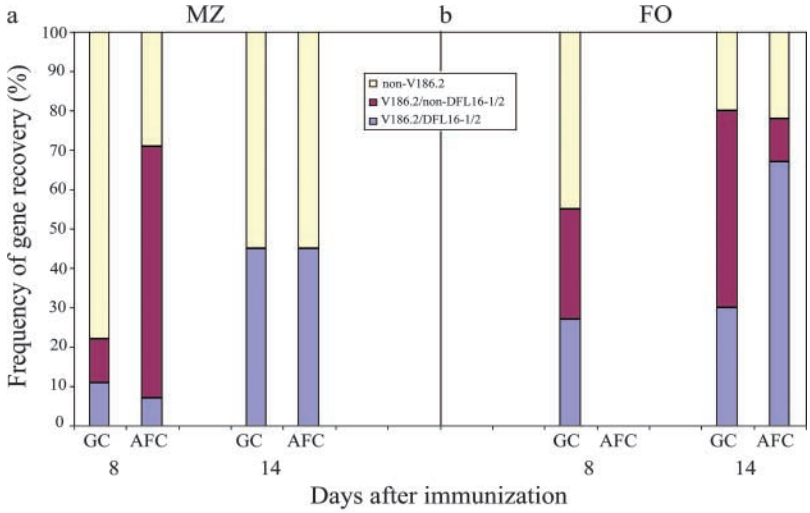

c

	CDR3													D Region	J_H
	98	99	100	101	102	103	104	105	106	107	108	109	110		
B1-8	AGA	TAC	GAT	TAC	TAC	GGT	AGT	AGC	TAC	TTT	GAC	TAC	TGG	DFL16.1	J_H2
1	---	---	---	AGT	AAC	TAC	GGA	CCC	---	---	---	---	---	un-identified	J_H2
2	---	---	---	AGT	AAC	TAC	GGA	CCC	---	---	---	---	---	un-identified	J_H2
3	---	---	---	AGT	AAC	TAC	GGA	CCC	---	---	---	---	---	un-identified	J_H2
4	---	---	---	AGT	AAC	TAC	GGA	CCC	---	---	---	---	---	un-identified	J_H2
5	---	---	---	AGT	AAC	TAC	GGA	CCC	---	---	---	---	---	un-identified	J_H2
6	---	---	---	AGT	AAC	TAC	GGA	CCC	---	---	---	---	---	un-identified	J_H2
7	---	---	---	AGT	AAC	TAC	GGA	CCC	---	---	---	---	---	un-identified	J_H2
8	---	---	---	AGT	AAC	TAC	GGA	CCC	---	---	---	---	---	un-identified	J_H2
9	---	---	TAT	GGT	AAC	TAC	GGT		---	---	---	---	---	DSP2-5/7	J_H2
10	---	---	TAT	GGT	AAC	TAC	GGT		---	---	---	---	---	DSP2-5/7	J_H2
11	---	---	TAT	GGT	AAC	TAC	GGT		---	---	---	---	---	DSP2-5/7	J_H2
12	---	---	TAT	GGT	AAC	TAC	GGT		---	---	---	---	---	DSP2-5/7	J_H2
13	---	TCG	GGC	TCA	GGC					---	---	---	---	un-identified	J_H2
14	---	TCG	GGC	TCA	GGC					---	---	---	---	un-identified	J_H2
15	---	TCG	GGC	TCA	GGC					---	---	---	---	un-identified	J_H2
16	---	TCG	GGC	TCA	GGC					---	---	---	---	un-identified	J_H2
17	---	TAT	AGA	CTA	ACT	GGG	ACG		---	---	---	---	---	un-identified	J_H2
18	---	TAT	AGA	CTA	ACT	GGG	ACG		---	---	---	---	---	un-identified	J_H2
19	---	TAT	AGA	CTA	ACT	GGG	ACG		---	---	---	---	---	un-identified	J_H2
20	---	TAT	AGA	CTA	ACT	GGG	ACG		---	---	---	---	---	un-identified	J_H2
21	---	GGG	GGG	TTT	ATT	ACT	ACG	GTA	GTA	GAA	AAC		---	un-identified	J_H2
22	---	GGG	GGG	TTT	ATT	ACT	ACG	GTA	GTA	GAA	AAC		---	un-identified	J_H2
23	---	AAG	GGG	GCT	GCA	GCC	CAG	GCC	CTT			---	---	un-identified	J_H2
24	---	---	---	--C	---		---	---	---	---	-A-	---	---	DFL16.1	J_H2
25	---	---	---	--C	---		---	---	---	---	-A-	---	---	DFL16.1	J_H2
26	---	---	---	--C	---		---	---	---	---	-A-	---	---	DFL16.1	J_H2
27	---	---	---	--C	---		---	---	---	---	-A-	---	---	DFL16.1	J_H2
28	---	---	---	--C	---		---	---	---	---	-A-	---	---	DFL16.1	J_H2
29	---	---	---	--C	---		---	---	---	---	-A-	---	---	DFL16.1	J_H2

Figure 6. Summary of V/D gene recovery from NP-reactive AFC and GC in mice reconstituted with MZ B cells plus T_H (a) or FO B cells plus T_H (b) at day 8 and day 14 after immunization with NP-CGG/alum. Between 400 and 600 clones from 10–15 independent PCR products were screened for V_H gene expression. The data are expressed as the percentage of cloned cells expressing V186.2/DFL16.1/2 rearrangements (blue), V186.2 rearranged to other D segments (red), and analogue V_H segments of the V186.2/V3 gene family (yellow). (c) Nucleotide sequences of V186.2/D rearrangements recovered from AFC foci on day 8 after the immunization in mice reconstituted with MZ B cells.

and/or affinity maturation. Therefore, it was important to assess whether the GCs in both MZ and FO mice supported somatic hypermutation in the V186.2$^+$ B cells. Other V_H clonotypes, which were identified by hybridization with a crossreactive DNA probe (see Materials and Methods) were not sequenced. As shown in Table III, ~60–70% of V186.2 sequences from day 8 GCs were mutated, with an average of 1.7 mutations/V_H in FO mice and 1.9 mutations/V_H in MZ mice. These numbers increased to 2.5 mutations/V_H and 2.8 mutations/V_H, respectively, by day 14, which is consistent with the mutation frequencies observed in the V186.2$^+$ GC B cells in NP-immunized intact C57BL/6 mice (20). There were high ratios of replacement to silent (R/S) mutations in CDR1 and 2, indicative of positive selection in both FO (R/S = 8) and MZ (R/S = 11) GCs (Table III, day 14).

On day 14, the majority of AFCs in both FO and MZ mice was somatically mutated (Table III) with high R/S ratios in CDRs and the canonical NP-specific mutation in V_H position 33 that replaces Trp(W) with Leu (L) (27), which are unmistakable signs of their origin from GC. Indeed, clonally related AFC and GC cells that shared somatic mutations were occasionally recovered from adjacent sites. In the case shown in Fig. 7, sequences from two foci, AFC-5 and AFC-20, shared four mutations with the adjacent GC-5, and shared five additional mutations with each other. The sequences from AFC-5 also contained seven unique mutations. Because of limited sampling, we cannot determine whether all AFC mutations occurred in the GC or whether the process of somatic hypermutation was perpetuated in the AFC focus.

Antibody Affinity and L Chain Repertoire. We next asked whether the distinctive repertoire of the early AFC response in MZ mice is reflected in the serum Ab quality. Unexpectedly, the NP-specific IgG in MZ mice had higher affinity on days 8 and 14, as indicated by the relative binding to NIP_4-BSA/NIP_{18}-BSA (Fig. 8 c). IgG from FO mice did not bind to NIP_4-BSA on day 8 and only matured a little by day 14.

Table III. *Somatic Mutations in VH186.2 Genes in FO- and MZ-derived AFC Foci and GC*

Cells sampled	Days after immunization	Recipients (mice/group)[a]	Number of sites sampled[b]	V_H186.2 sequences		Mutations/V_H (average)	W33L mutation[c]	R|S[d]	
				Total	Mutated (%)			CDR1 + 2	FW
AFC foci	8	FO (2 mice)	ND						
		MZ (2 mice)	1	12	0	0	0		
			2[e]	10	0	0	0		
			1[e]	8	60	1.2	0		
	14	FO (2 mice)	3	20	85	1.5	12	10.0	1.7
		MZ (3 mice)	4	18	95	1.6	7	8.0	1.7
GC	8	FO (2 mice)	4	25	62	1.7	0		
		MZ (2 mice)	2	14	75	1.9	0		
	14	FO (2 mice)	7	32	90	2.5	8	8.0	1.4
		MZ (3 mice)	4	13	100	2.8	0	11.0	2.1

[a]Number of *scid* mice reconstituted with either FO B cells or MZ B cells plus T_H cells and sacrificed on the indicated day after immunization with NP-CGG.
[b]At least one focus (~20–50 AFC) and one GC was microdissected from each spleen.
[c]Number of sequences with tryptophan → leucine replacement in V_H position 33.
[d]Replacement/silent mutation ratio.
[e]These foci were dissected from the same spleen.

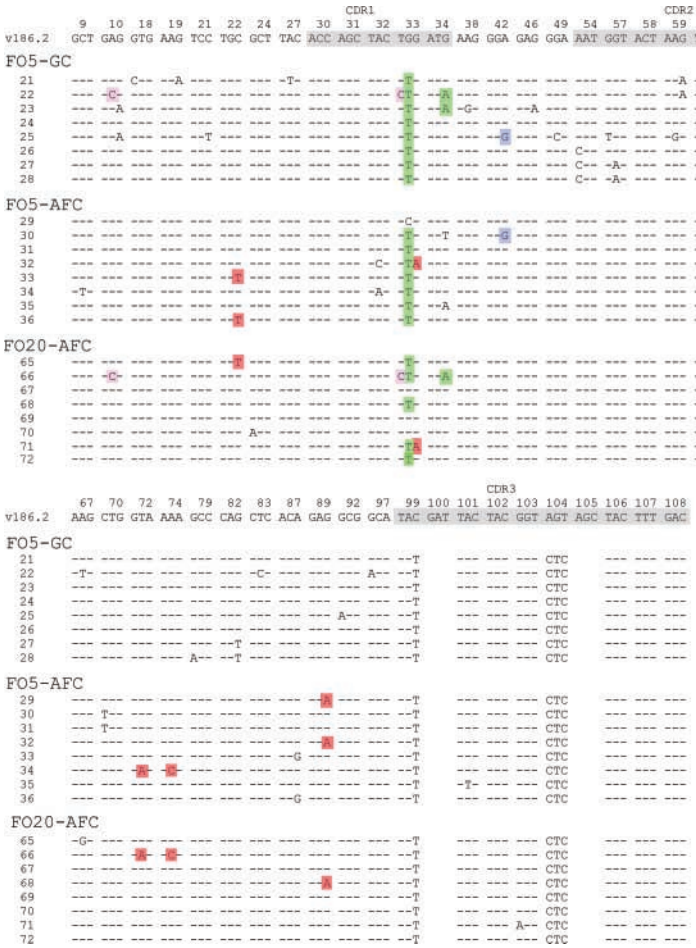

Figure 7. V186.2/DFL16.2 nucleotide sequences recovered from adjacent GC #5 and AFC foci #5 and #20 in mice reconstituted with FO B cells on day 14 after the immunization. Colored bases indicate common point mutations that were found in sequences from all three sites (green) and those found in GC #5 and AFC #5 (blue), GG #5 and AFC #20 (purple), and AFC #5 and AFC #20 (orange).

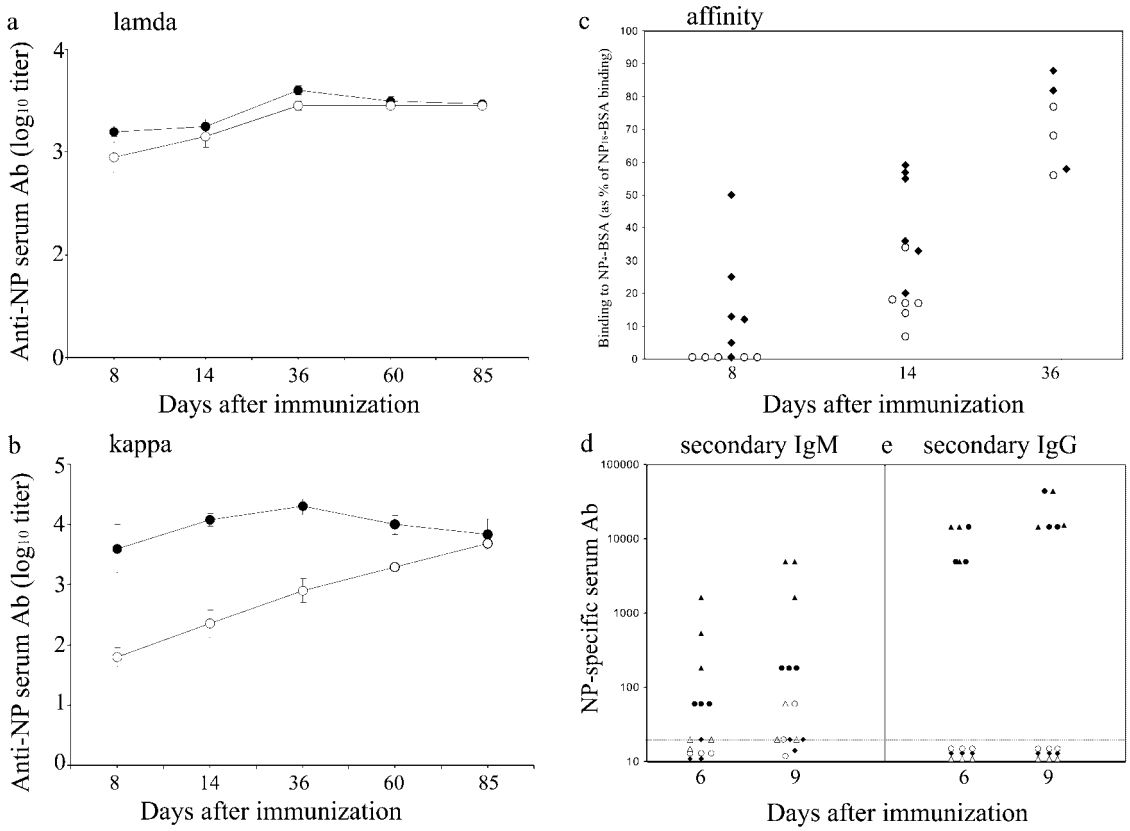

Figure 8. Light chain usage (a and b), antibody affinity (c), and anamnestic response (d and e) in mice reconstituted with MZ and FO B cells. Total anti-NP serum antibody with lambda (a) and kappa (b) light chains in mice reconstituted with MZ cells (●) or FO cells (○) (mean titer in three to seven mice per interval ± SD). Relative affinities of anti-NP serum IgG1 Ab in mice reconstituted with MZ B cells + T_H (◆) or FO B cells + T_H (○) were determined at various intervals after the immunization with NP-CGG (see Materials and Methods). Zero values show the IgG1 with no binding to NP_4-BSA (c). Secondary anti-NP IgM (d) and IgG (e) serum Ab titers in *scid* mice reconstituted with spleen cells from various donors: antigen-primed MZ mice (▲ and Δ), antigen-primed FO mice (● and ○), or normal, naive BL/6 mice (◆). Each symbol indicates one recipient. The recipients were either challenged with 10 μg of soluble NP-CGG (▲, ●, and ◆) or not (Δ and ○).

The Abs from both groups reached nearly equivalent binding to NIP_4/NIP_{18} after 1 mo. The anti-NP antibody in MZ and FO mice also differed in the L chain isotype. Although Abs with lambda chain were prevalent in both groups (Fig. 8 a), the MZ mice had ~2 log higher titers of kappa$^+$ anti-NP Ab than the FO mice (Fig. 8 b); the two groups reached similar levels of kappa$^+$ Ab after 2 mo. An increased proportion of kappa$^+$ Ab is typical of the late primary or secondary response to NP (31). Together, the noncanonical CDR3 repertoire of AFC, the higher affinity of early Ab, and the higher proportion of kappa$^+$ Ab suggest that the rapidly responding NP-specific MZ B cells had been immunologically preselected for their role in early responses.

Anamnestic IgM and IgG Responses. Lastly, we examined whether the mice reconstituted with either MZ or FO B cells and primed with NP-CGG/alum developed immunological memory. Both groups maintained high titers of anti-NP IgG even at 3 mo after the immunization, which could have masked the de novo response to Ag boost. Therefore, the splenocytes from the NP-CGG–primed MZ and FO mice were adoptively transferred into C57BL/6/*scid* recipients, and the recipients were challenged with 10 μg of NP-CGG in PBS. An administration of low dose of soluble NP-CGG induces a rapid, anamnestic Ab response in mice that were primed with Ag in alum adjuvants, but it does not elicit an appreciable Ab response in naive mice. Note that the *scid* recipients of splenocytes from unprimed donors indeed failed to mount any IgM (Fig. 8 d) or IgG (Fig. 8 e) Ab response to the boost with 10 μg of soluble NP-CGG. In contrast, the recipients of Ag-primed lymphocytes from either MZ or FO donors responded to the challenge by a brisk anamnestic IgG response that was comparable in kinetics and magnitude (Fig. 8 e). Surprisingly, the recipients of primed MZ cells (but not FO) also mounted a rapid IgM response (Fig. 8 d), which was not seen with naive cells (not depicted), indicating that the proclivity of MZ B cell for IgM production is maintained even in the long-term memory cell population.

Discussion

We have delineated the functional differences and similarities between MZ and FO B cells in response to a TD antigen in vivo. We demonstrate, for the first time, that

hapten-reactive MZ B cells are functionally and clonally heterogeneous and that they are capable of forming GCs. Although the bulk of the early primary response by MZ and FO is skewed to the AFC and GC formation, respectively, evidence is provided that the functions of these two cell subsets, in fact, overlap.

MZ B cells have been identified previously as a primary source of early AFC response to TI Ags (8). The potential role of these cells in response to TD hapten–protein conjugates was explored by Liu et al. (19) using immunohistological techniques. In their view, the Ag challenge induced a rapid movement of hapten-specific B cells into the MZ where they differentiated into hapten-binding cells, which were regarded as likely candidates for transport of immune complexes back to the follicles. However, the hapten-binding MZ B cells appeared to have no relationship to the plasmacytes that arose concurrently in the splenic red pulp. We now provide direct evidence that MZ B cells are the major source of the early primary AFC plasmacytes in response to a TD Ag.

The repertoire of the rapid MZ AFC response to NP had several unexpected features. The usage of V_H186.2 gene was higher than that typically observed in the primary GC (20, 26; Fig. 6 a), however, this V_H segment was rarely joined to the DFL16.1/2 gene, contrary to the canonical V186.2/DFL16.1 rearrangements that are found later in the NP-driven response (21–23; Fig. 6, a and b). Interestingly, the use of noncanonical D segments was shown to be a characteristic of secondary anti-NP repertoire based on analysis of hybridomas (21). Here we show that in addition to the unique VD repertoire, the early MZ-derived AFC contained occasional point mutations in the V_H gene and produced circulating IgG Ab that had higher antibody affinity for NP than the primary IgG Ab produced by FO B cells. These results suggest that the first wave of AFC arises from a subset of NP-reactive B cells that have been selected into MZ pool by stimulation with an NP-crossreactive epitope, either a self-ligand (3) or an environmental Ag. We hypothesize that this "natural priming" fortuitously stimulates an expansion of cell clones that react with NP more avidly than the naive NP-specific B cells. The theory that the BCR of these cells use kappa light chains instead of lambda may be conjectured from the observation of higher levels of kappa$^+$ anti-NP Ab in the MZ mice (Fig. 8 b).

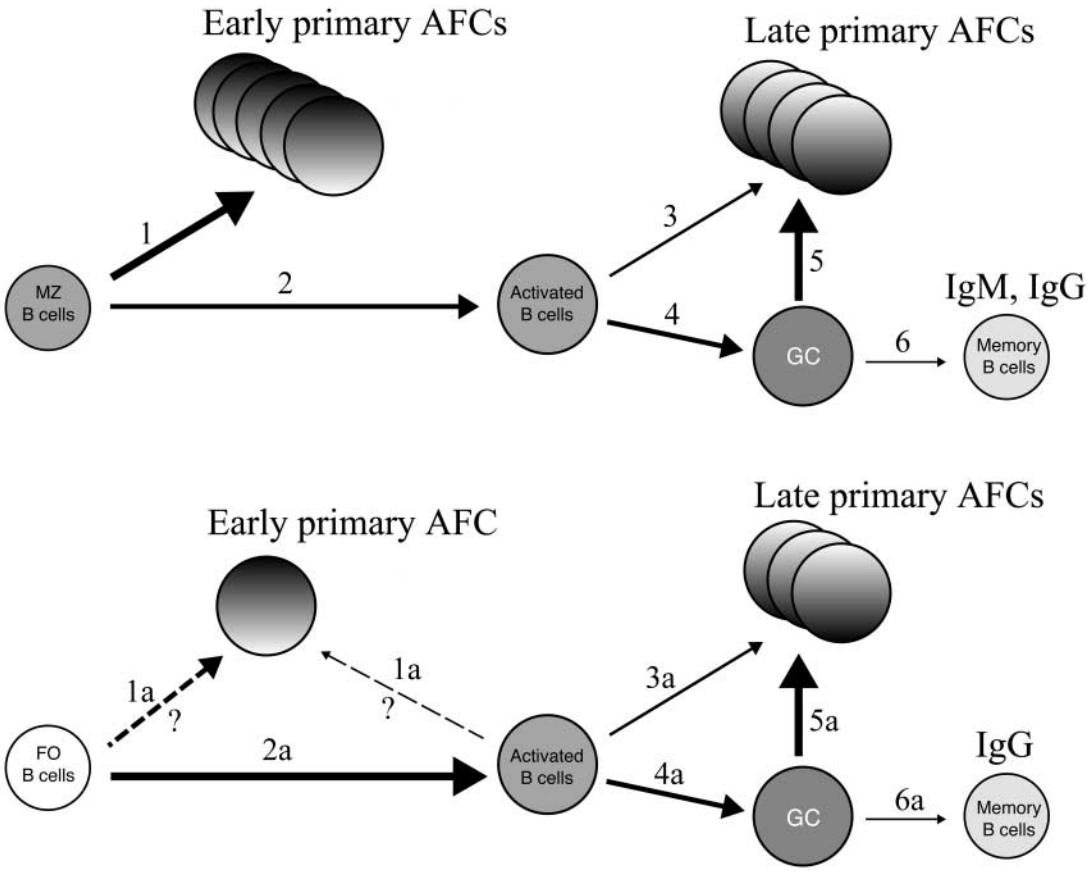

Figure 9. Working model of splenic B cell responses to a TD antigen. Antigen-reactive ("naturally primed") MZ B cells produce the large foci of early AFCs (1) similar to the model of TI response in reference 5. Clonotypically distinct MZ B cells become activated (2) and either enter GC (4) or differentiate into late AFC (3); the majority of late AFCs derive from GC (5). MZ-derived memory cells (6) produce anamnestic IgM and IgG Ab upon restimulation. FO B cells are the main source of GC (2a and 4a), producing late AFCs either directly (3a) or from GC (5a) and generating IgG-producing memory B cells (6a). Early AFC may be formed either by an FO B cell subset or by the GC-committed population (1a).

The adoptive cell transfer system revealed the potential of purified MZ B cells to generate conventional GC upon stimulation with TD Ag in the presence of Ag-primed T_H cells. Up to 20% of B cells in the recipient spleen expressed the GL-7 marker of GC, which is within the upper ranges of GC reaction reported in other studies (27, 32). Using B cell subsets expressing different Ly5 alleles, we showed that the majority of GCs in MZ-reconstituted mice came from the MZ cells rather than from contaminating immature cells and that MZ B cells were able to generate the GL-7^+ GC cells even in the presence of excess FO B cells. In chimeras that received Ly5.2^+ MZ and Ly5.1^+ FO cells, individual PNA^+ splenic GC were entirely either Ly5.1 positive or negative. We have not observed a mosaic staining pattern with a mixture of $PNA^+Ly5.1^-$ and $PNA^+Ly5.1^+$ cells within a GC (Fig. 4), suggesting that individual centers were founded either by MZ or FO B cell precursors, consistent with the theory of a pauciclonal origin of GC (20). Thus, our data clearly demonstrate that MZ B cells are functionally heterogeneous, containing distinct precursors for the rapid AFC formation and for GC formation (Fig. 9). When BCR on MZ cells binds Ag, they move rapidly to the splenic T cell zones (4, 33). We conjecture that some of these cells receive helper signals for migration to follicles and GC formation (Fig. 9).

It was surprising that MZ B cells, despite their rapid switch from IgM to IgG, continued to produce high levels of IgM Ab during a 3-mo period after the immunization and that they could also produce a robust rapid IgM anamnestic response. This implies that a significant proportion of Ag-stimulated MZ B cells does not undergo class-switch recombination (CSR) and that the cells remain at the VDJ/μ configuration even during their differentiation into memory B cells in GC. An induction of a robust IgM memory by priming with TD antigens has been observed previously (34, 35); our results now identify MZ B cells as the source of this IgM memory. It may be that MZ B cells respond less well to TD signals (cytokines or cognate stimuli) that are presumably required for the accessibility of DNA for CSR downstream of Cμ (36). An alternative mechanism for the long-term IgM-producing B cells is suggested from the recent demonstration by Dudley et al. (37) that increased activity of AID, an enzyme required for CSR, may lead to deletion of the 5′ internal switch μ sequence in some IgM-producing B cells, thus preventing any further isotype switch. We hypothesize that this mechanism occurs in the "naturally activated" MZ B cells but not in the FO B cells.

The working model in Fig. 9 proposes that the FO cells are committed mainly to GC formation and the late primary AFC. It is not clear whether the first anti-NP serum Ab in FO cell–reconstituted mice originated from the rapidly expanding GC or from an independent, small population of AFC precursors (Fig. 9, 1a). Still, the model of TD response in Fig. 9 emphasizes distinction between the earliest wave of AFC from MZ B cells and the later AFC that were produced by both MZ and FO cells, which had a V_H gene repertoire similar to that of respective GC. Clonally related cells with shared point mutations were readily recovered from AFC foci and GC on day 14, indicating that the AFCs originated from those B cells within GCs that up-regulate Blimp-1 and differentiate into plasmacytes (38) (Fig. 9, 5 and 5a). However, a proportion of the late AFCs was unmutated; yet, some of them may also share CDR3 with GC B cells (39). This suggests that daughters of single, antigen-driven MZ and FO B cells may either form GCs and/or become plasmacytes (Fig. 9, 3, 3a, 4, and 4a).

Our results support the notion that the response of MZ B cells to a single epitope, NP, can be heterogeneous both functionally and clonotypically. Further studies are needed to test the hypothesis that MZ B cells include distinct clones, either which produce the rapid AFC response or those with different genealogy and genetic program that form the GC.

The authors are grateful to Dr. Martin Flajnik and Dr. Ferenc Livak for critical reading and editing of the manuscript and to Ms. Karen Chadwick (Johns Hopkins University, School of Hygiene, Baltimore, MD) for her expert help on FACS® sorting.

Submitted: 29 August 2003
Accepted: 6 November 2003

References

1. Maclennan, I.C.M. 1998. B cell receptor regulation of peripheral B cells. *Curr. Opin. Immunol.* 10:220–225.
2. Kantor, A.B., and L.A. Herzenberg. 1993. Origin of murine B cell lineages. *Annu. Rev. Immunol.* 11:501–538.
3. Martin, F., and J.F. Kearney. 2002. Marginal zone B cells. *Nat. Immunol. Rev.* 2:323–333.
4. Gray, D., I.C.M. Maclennan, H. Bazin, and M. Khan. 1982. Migrant $\mu^+\delta^+$ and static $\mu^+\delta^-$ B lymphocyte subsets. *Eur. J. Immunol.* 12:564–569.
5. Oliver, A.M., F. Martin, and J.F. Kearney. 1999. IgM^{hi} $CD21^{hi}$ lymphocytes enriched in the splenic marginal zone generate effector cells more rapidly than the bulk of follicular B cells. *J. Immunol.* 162:7198–7207.
6. Oliver, A.M., F. Martin, G.L. Gartland, R.H. Carter, and J.F. Kearney. 1997. Marginal zone B cells exhibit unique activation, proliferative and immunoglobulin secretion responses. *Eur. J. Immunol.* 27:2366–2374.
7. Snapper, C.M., H. Yamada, D. Smoot, R. Sneed, A. Lees, and J.J. Mond. 1993. Comparative in vitro analysis of proliferation, Ig secretion, and Ig class switching by murine marginal zone and follicular B cells. *J. Immunol.* 150:2737–2745.
8. Martin, F., A.M. Oliver, and J.F. Kearney. 2001. Marginal zone B and B1 B cells unite in the early response against T-independent blood-borne particulate antigens. *Immunity.* 14:617–629.
9. Loder, F., B. Mutschler, R.J. Ray, C.J. Paige, P. Sideras, R. Torres, M.C. Lamers, and R. Carsetti. 1999. B cell development in the spleen takes place in discrete steps and is determined by the quality of B cell receptor-derived signals. *J. Exp. Med.* 190:75–89.
10. Wang, J.H., N. Avitahl, A. Cariappa, C. Friedrich, T. Ikeda, A. Renold, K. Andrikopoulos, L. Liang, S. Pillai, B.A. Morgan, and K. Georgopoulos. 1998. *Aiolos* regulates B cell acti-

vation and maturation to effector state. *Immunity.* 9:543–553.
11. Martin, F., and J.F. Kearney. 2000. Positive selection from newly formed to marginal zone B cells depends on the rate of clonal production, CD19, and btk. *Immunity.* 12:39–49.
12. Tange, S.G., Y.-J. Liu, G. Aversa, J.H. Phillips, and J.E. de Vries. 1998. Identification of functional human splenic memory B cells by expression of CD148 and CD27. *J. Exp. Med.* 188:1691–1703.
13. Klein, U., K. Rajewky, and R. Kuppers. 1998. Human immunoglobulin IgM^+/IgD^+ peripheral blood B cells expressing the CD27 cell surface antigen carry somatically mutated variable region genes: CD27 as a general marker for somatically mutated (memory) B cells. *J. Exp. Med.* 188:1679–1689.
14. Dammers, P.M., A. Visser, E.R. Popa, P. Nieuwenhuis, and F.G. Kroese. 2000. Most marginal zone B cells in rat express germline encoded IgVH genes and are ligand selected. *J. Immunol.* 165:6156–6169.
15. Fagarasan, S., and T. Honjo. 2000. T-independent immune response: new aspects of B cell biology. *Science.* 290:89–92.
16. Guinamard, R., M. Okigaki, J. Schlessinger, and J.V. Ravetch. 2000. Absence of marginal zone B cells in Pyk-2-deficient mice defines their role in the humoral response. *Nat. Immunol.* 1:31–36.
17. Tanigaki, K., H. Han, N. Yamamoto, K. Tashiro, M. Ikegawa, K. Kuroda, A. Suzuki, T. Nakano, and T. Honjo. 2002. Notch-RBP-J signaling is involved in cell fate determination of marginal zone B cells. *Nat. Immunol.* 3:443–449.
18. Maclennan, I.C.M. and Y.-J. Liu. 1991. Marginal zone B cells respond both to polysaccharide antigens and protein antigens. *Res. Immunol.* 142:346–351.
19. Liu, Y.-J., S. Oldfield, and I.C.M. Maclennan. 1988. Memory B cells in T-dependent antibody responses colonize the splenic marginal zones. *Eur. J. Immunol.* 18:355–362.
20. Jacob, J., J. Przylepa, C. Miller, and G. Kelsoe. 1993. In situ studies of the primary immune responses to (4-hydroxy-3-nitrophenyl) acetyl. III. The kinetics of V-region mutation and selection in germinal center B cells. *J. Exp. Med.* 178: 1293–1307.
21. Cumano, A., and K. Rajewsky. 1986. Clonal recruitment and somatic mutation in the generation of immunologic memory to the hapten NP. *EMBO J.* 5:2459–2468.
22. Bothwell, A.L.M., M. Paskind, M. Reth, T. Imanishi-Kari, K. Rajewsky, and D. Baltimore. 1981. Heavy chain variable region contribution to the NPb family of antibodies: Somatic mutation evident in a gamma 2a variable region. *Cell.* 24: 625–637.
23. Bothwell, A.L.M., M. Paskind, M. Reth, T. Imanishi-Kari, K. Rajewsky, and D. Baltimore. 1982. Somatic variants of murine immunoglobulin lambda light chains. *Nature.* 298: 380–382.
24. Weinberger, J.Z., M.I. Green, B. Benaceraf, and M.E. Dorf. 1979. Hapten-specific T cell responses to 4-hydroxy-3-nitrophenyacetyl. I. Genetic control of delayed-type hypersensitivity by V and I-A region genes. *J. Exp. Med.* 149:1336–1348.
25. Yang, X., J. Stedra, and J. Cerny. 1996. Relative contribution of T and B cells to hypermutation and selection of the antibody repertoire in germinal centers of aged mice. *J. Exp. Med.* 183:959–966.
26. Nie, X., S. Basu, and J. Cerny. 1997. Immunization with immune complex alters the repertoire of antigen-reactive B cells in the germinal centers. *Eur. J. Immunol.* 27:3517–3525.
27. McHeyzer-Williams, M.G., M.J. Mclean, P.A. Lalor, and G.J. Norssal. 1993. Antigen-driven B cell differentiation in vivo. *J. Exp. Med.* 178:295–307.
28. Stedra, J., and J. Cerny. 1994. Distinct pathways of B cell differentiation. I. Residual T cells in athymic mice support the development of splenic germinal centers and B cell memory without an induction of antibody. *J. Immunol.* 152:1718–1726.
29. Miller, C., J. Stedra, G. Kelsoe, and J. Cerny. 1995. Facultative role of germinal centers and T cells in the somatic diversification of IgV_H genes. *J. Exp. Med.* 181:1319–1331.
30. Fehr, T., R.C. Rickert, B. Odermatt, J. Roes, K. Rajewsky, H. Hengartner, and R.M. Zinkernagel. 1998. Antiviral protection and germinal center formation but impaired B cell memory in the absence of CD19. *J. Exp. Med.* 188:145–156.
31. Reth, M., G.J. Hammerling, and K. Rajewsky. 1978. Analysis of the repertoire of anti-NP antibodies in C57BL/6 mice by cell fusion. I. Characterization of antibody families in the primary and hyperimmune responses. *Eur. J. Immunol.* 8:393–400.
32. Coico, R.F., B.S. Bhogal, and G.J. Thorbecke. 1983. Relationships of germinal centers in lymphoid tissue to immunologic memory. IV. Transfer of B cell memory with lymph node cells fractionated according to their receptor for peanut agglutinin. *J. Immunol.* 131:2254–2257.
33. Vinuesa, C.G., Y. Sunners, J. Pongracz, J. Ball, K.M. Toellner, D. Taylor, I.C.M. MacLennan, and M.C. Cook. 2001. Tracking the response of Xid B cells *in vivo*: T1-2 antigen induces migration and proliferation but Btk is essential for terminal differentiation. *Eur. J. Immunol.* 31:1340–1350.
34. Valentova, V., J. Cerny, and J. Ivanyi. 1966. Characterization of the immunological memory of the IgM type of response in chickens. *Folia Biologica.* 12:207–211.
35. Nossal, G.J.V., C.M. Austin, and J.L. Ada. 1965. Antigens in immunity. VII. Analysis of immunological memory. *Immunology.* 9:333–348.
36. Snapper, C.M., and F.D. Finkelman. 1998. Immunoglobulin class switch. *In* Fundamental Immunology. Fourth edition. W.E. Paul, editor. Lippincott-Raven Publishers, Philadelphia, PA/New York. 831–862.
37. Dudley, D.D., J.P. Manis, A.A. Zarrin, L. Kaylor, M. Tian, and F.W. Alt. 2002. Internal IgH class switch region deletions are position-independent and enhanced by AID expression. *Proc. Natl. Acad. Sci. USA.* 99:9984–9989.
38. Angelin-Duclos, C., C. Giorgio, K.-I. Lin, and K. Calame. 2000. Commitment of B lymphocytes to a plasma cell fate is associated with Blimp-1 expression in vivo. *J. Immunol.* 165: 5462–5471.
39. Jacob, J., and G. Kelsoe. 1992. In situ studies of the primary immune response to (4-hydroxy-3-nitrophenyl) acetyl. II. A common clonal origin for periarteriolar lymphoid sheath-associated foci and germinal centers. *J. Exp. Med.* 176:679–687.